

Dynamics of spin-torque oscillators in vortex and uniform magnetization state

R. Lehndorff¹, D. E. Bürgler¹, S. Gliga¹, R. Hertel¹, P. Grünberg¹, C. M. Schneider¹, Z. Celinski²

¹ IFF-9: Electronic Properties

² Center for Magnetism and Magnetic Nanostructures, University of Colorado at Colorado Springs, USA

Current-driven magnetization dynamics in spin-torque oscillators (STO) has a high potential for high-frequency (HF) applications. We experimentally study current-driven HF excitations of STOs in the vortex and uniform in-plane magnetized state. Our ability to switch between these two states in a given STO enables a direct comparison of the STO characteristics. We find that the vortex state maximizes the emitted HF power and shows a wider frequency tuning range.

Spin-torque oscillators (STO) based on ferromagnet/non-magnet/ferromagnet ($\text{FM}_{\text{fixed}}/\text{NM}/\text{FM}_{\text{free}}$) layered structures are an application of current-induced magnetization dynamics. They show a steady precession of the magnetization of FM_{free} under the action of a spin-polarized DC current. This precession generates via the giant or tunnel magnetoresistance (GMR, TMR) effect a HF voltage oscillation with frequencies in the GHz range, which can be tuned by the DC current amplitude and the external magnetic field strength. Still, one drawback of STOs is their low output power. Several groups work on the synchronization of arrays of STOs in order to achieve useful power levels. While this is a very promising approach, maximizing the output power of every single STO is undeniably the first step to do.

There are several possible arrangements for STOs, e.g. with in-plane, out-of-plane, or vortex-type magnetized FM_{fixed} and/or FM_{free} . Comparing the characteristics of HF excitations – especially output power – from different experiments is not conclusive, because impedance and absolute resistance variations of the samples strongly influence the detected power. Here, we study HF excitations in two mentioned arrangements that we are able to realize in the same STO. While FM_{fixed} is uniformly in-plane magnetized, FM_{free} is either uniformly in-plane magnetized or in a vortex state. The direct comparison shows some advantages of the vortex state for the application of STOs [1].

Samples are fabricated by depositing 150 nm Ag/ 2 nm Fe/ 6 nm Ag/ 20 nm Fe/ 50 nm Au by molecular beam epitaxy on GaAs(100). The nanopillars are defined by electron beam lithography and ion beam etching and have a circular cross section with a diameter of 230 nm. Only the top magnetic layer (FM_{free}) is laterally confined, while the bottom layer (FM_{fixed})

is extended with a typical width of $15\ \mu\text{m}$ (see inset in Fig. 1). The dimensions of FM_{free} are in a regime where a magnetic vortex and a uniform in-plane magnetization are both stable states [2]. The 2 nm-thick FM_{fixed} is uniformly magnetized on length scales much larger than the pillar diameter as long as a small magnetic field suppresses domain formation.

Figure 1 shows current-perpendicular-plane (CPP) GMR curves at 10 K with the magnetic field applied in the sample plane. Starting from saturation at 150 mT (blue curve) FM_{free} and FM_{fixed} undergo a gradual change from parallel to antiparallel alignment due to stray field interaction. The completely antiparallel alignment is reached at 0 mT and results in a high resistance. FM_{free} shows a uniform in-plane magnetization in this field range. After field reversal at about -20 mT in the formation of a vortex in FM_{free} results in a drop of the resistance. Upon further sweeping the field, the vortex core is moved from the center of the disk to the rim until it is expelled at about -100 mT. Micromagnetic simulations qualitatively reproduce this behavior as shown by the magnetization patterns in Fig. 1 (for more details see [1]).

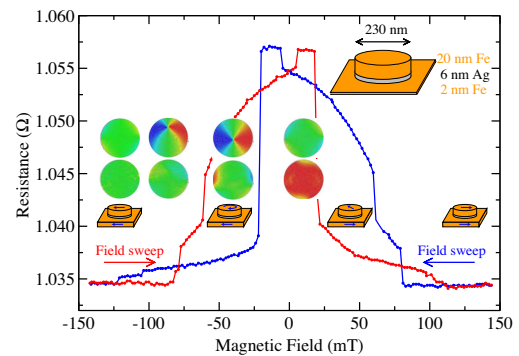


FIG. 1: CPP-GMR curves for increasing and decreasing field. Symbols and simulated micromagnetic magnetization patterns for FM_{fixed} (bottom) and FM_{free} (top) correspond to the decreasing (blue) sweep direction.

Figure 2 shows current-induced CPP resistance changes at 10 K and various field strengths. The initial states were prepared by magnetic field sweeps according to Fig. 1. We observe hysteretic switching of FM_{free} (e.g. green and red curves). The high-resistive state at positive currents corresponds to uniformly and antiparallely aligned magnetizations in

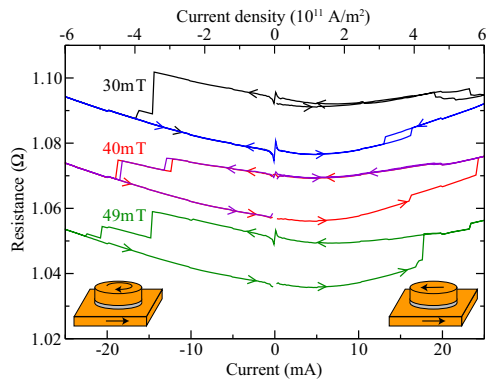


FIG. 2: Current-induced switching between the low-resistive vortex and high-resistive uniform state. The black and purple curves start in the uniform state, all others in the vortex state. For clarity the graphs measured at 40 and 30 mT are offset by +20 and +40 mΩ, respectively.

FM_{free} and FM_{fixed} , whereas the low-resistive state at negative currents is due to the vortex state in FM_{free} . This is in agreement with previous experiments on Fe/Ag/Fe nanopillars [3], which have established that the spin-transfer torque due to a positive current acts towards an antiparallel alignment. The fact that we do not observe a switching to the vortex state at positive currents in Fig. 2 proves that the prevalent torque in the switching processes does not originate from Oersted fields. These circumferential fields tend to switch the magnetization of FM_{free} into a vortex state also at positive currents, just with the opposite vorticity compared to negative currents.

We measure DC current-induced HF excitations of the magnetization at room temperature by amplification and detection of voltage oscillations across the nanopillar using a microwave probe station. The voltage variation arises from the GMR of the Fe/Ag/Fe stack, which reaches 2% or 22 mΩ in Fig. 1. The impedance of our sample was 11 Ω at 1.5 GHz. Figure 3(a) shows the HF response of a STO in the uniform state measured in an in-plane field of 82 mT. The low frequencies of the excitations are the result of the cancellation of the dipolar coupling field of about 80 mT by the external field and the rather large size of the element, for which the standing-wave mode has a low frequency. The observed blue-shift behavior at low currents can be interpreted in terms of standing-wave modes, which are deformed by the Oersted field. At higher currents the red-shift sets in that is explained by a predominantly homogeneous in-plane precession of the magnetization. Figure 3(b) shows representative HF excitations of a STO in the vortex state. Here, the gyrotropic mode [4] of the vortex is excited as previously reported by Pribiag *et al.* [5]. The gyrotropic mode is the lowest excitation mode of a magnetic vortex and consists of a circular motion of the vortex core around the equilibrium position. The radius of the trajectory is proportional to the excitation amplitude. When for increasing current the trajectory approaches the rim of the disk, the vortex experiences a stronger restoring force, increasing its precessional frequency. This results in a linear

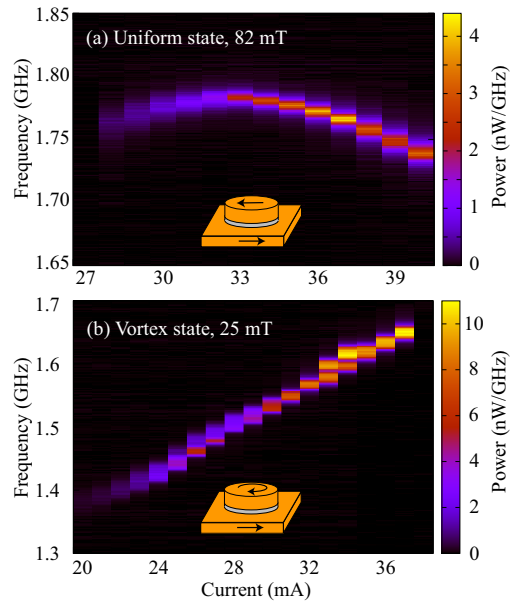


FIG. 3: Spin-transfer torque induced excitation of qualitatively different oscillatory modes in a STO: (a) Standing-wave mode in the uniform state and (b) gyrotropic mode of the vortex state. The microwave power generated by the gyrating vortex for a given DC current in (b) is much higher than for the standing-wave mode in (a).

increase of the frequency yielding a mode agility of +17 MHz/mA [Fig. 3(b)]. At each spot within the trajectory of the vortex core, the magnetization rotates during one period of the gyrotropic cycle by full 2π about the sample normal. Thus, for a vortex core moving on a trajectory close to the rim of the sample the product of oscillation amplitude times area, where oscillations take place, is maximized. As a consequence, the emitted power of the STO in the vortex state is nearly three times the power emitted in the uniform state (Fig. 3).

In conclusion, we directly compared the characteristics of a STO in either the uniform state or the vortex state. Higher agility, wider tuning range, and higher output power are all advantageous for the application of the vortex state in STOs. Although this conclusion is derived from metallic, GMR-type STOs, our generic, micromagnetic arguments are also valid for the technologically more relevant TMR-based STOs.

- [1] R. Lehdorff, D. E. Bürgler, S. Gliga, R. Hertel, P. Grünberg, C. M. Schneider, and Z. Celinski, Phys. Rev. B **78**, 054412 (2009).
- [2] R. P. Cowburn, J. Phys. D: Appl. Phys. **33**, R1 (2000).
- [3] R. Lehdorff, M. Buchmeier, D. E. Bürgler, A. Kakay, R. Hertel, and C. M. Schneider, Phys. Rev. B **76**, 214420 (2007).
- [4] K. Y. Guslienko, B. A. Ivanov, V. Novosad, Y. Otani, H. Shima, and K. Fukamichi, J. Appl. Phys. **91**, 8037 (2002).
- [5] V. S. Pribiag, I. N. Krivorotov, G. D. Fuchs, P. M. Braganca, O. Ozatay, J. C. Sankey, D. C. Ralph, and R. A. Buhrman, Nature Physics **3**, 498 (2007).